Journal of the European Ceramic Society **14** (1994) 227–235

Grain Boundary Modifications of Manganese Ferrites

Jeffrey H. Boy* & Gerald P. Wirtz

Department of Material Science and Engineering, University of Illinois at Urbana, Champaign, Urbana, Illinois 61801, USA

(Received 15 September 1993; accepted 18 January 1994)

Abstract

The effect of minor additions (<1 wt%) of SiO_2 and $CaCO_3$ to manganese ferrites was investigated. Complex impedance analysis showed that the resistivity was modified by altering the electrical response of the grain boundaries. The measured resistivity of the grain boundaries went through a maximum at between 0·2 and 0·4 wt% additions. DC conductivity measurements showed a shift from grain boundary to bulk control of the conductivity at fields $>10^3$ V/m. An equivalent circuit model was used to calculate the coefficient of non-ohmic response for Mn ferrites which were less than 3·0 for all compositions investigated. Differential thermal analysis in a magnetic field showed that Mn ferrite decomposed when subjected to post sintering thermal anneals at temperatures >600°C in air. The addition of less than 1 wt% SiO_2 and $CaCO_3$ inhibited this phase decomposition, by preventing the rapid diffusion of oxygen at the grain boundaries. The control of oxidation in ferrites by dopants is in addition to the previously recognized role in the control of the electrical and magnetic properties.

Der Effekt der Zugabe (< 1 Gew%) von SiO_2 und $CaCO_3$ zu Manganferriten wurde untersucht. Die Untersuchung der Wechselstromimpedanz zeigte, daß sich der Widerstand durch das unterschiedliche Verhalten der Korngrenzen veränderte. Der gemessene Widerstand der Korngrenzen ging durch ein Maximum bei Zugaben zwischen 0·2 und 0·4 Gew%. Die Gleichstromleitfähigkeit veränderte sich von Korngrenzen- zu Materialleitfähigkeit bei einer Feldstärke > 10^3 V/m. Mit Hilfe eines Äquivalentschaltkreismodells wurde der Koeffizient des Nicht-Ohmschen-Verhaltens der Mn-Ferrite berechnet. Der Koeffizient war für alle untersuchten Verbunde kleiner als 3·0. Die Differentialthermoanalyse in einem magnetischen Feld ergab, daß Mn-Ferrite zerfallen, wenn sie nach dem Sintern bei Temperaturen > 600°C an Luft wärmebehandelt werden. Die Zugabe von weniger als 1 Gew% SiO_2 und $CaCO_3$ hemmte den Zerfall dieser Phase durch das Verhindern der schnellen Sauerstoff-diffusion entlang der Korngrenzen. Die Kontrolle der Oxidation in Ferriten durch Dotierung ist ein neuer Aspekt, der zusätzlich zu der bereits bekannten Rolle, die die Dotierung bei der Kontrolle der elektrischen und magnetischen Eigenschaften spielt, gefunden wurde.

On a étudié l'effet de faibles additions (<1%pond) de SiO_2 et $CaCO_3$ dans des ferrites de manganèse. L'analyse de l'impédance complexe montre que la réponse électrique des joint de grains a été modifiée, changeant ainsi la résisitivité. La résistivité des joints de grains, d'après les mesures, passe par un maximum pour une teneur comprise entre 0·2 et 0·4%. Les mesures de conductivité en courant continu mettent en évidence le passage d'une conductivité controlée par les joints à une conductivité controlée par le volume, pour des champs $>10^3$ V/m. On a calculé le coefficient de réponse non-ohmique pour les ferrites de manganèse à l'aide d'un modèle de circuit équivalent: on trouve des valeurs inférieures à 3·0 pour toute les compositions étudiées. L'analyse différentielle thermique sous champ magnétique montre que la ferrite de manganèse se décompose lorsqu'on la soumet, après frittage, a des recuits sous air à T>600°C. En ajoutant une quantité de SiO_2 et $CaCO_3$ inférieure à 1% pond, on peut éviter cette décomposition, en empêchant la diffusion rapide de l'oxygène aux joints de grains. Ainsi l'addition de dopants permet non seulement de contrôler les propriétés électriques et magnétiques, ce qui etait déjà admis, mais aussi de contrôler l'oxydation.

1 Introduction

During the last 30 years there has been an increased recognition of the importance of grain

* Present address: US Army Corps of Engineers, Construction Engineering Research Laboratories, Champaign, Illinois 61826, USA.

boundaries in determining the electrical properties of oxide ceramics.[1,2] This has lead to further recognition that grain boundaries can be engineered to yield new devices with unique properties such as (1) internal boundary layer capacitors, $SrTiO_3$ based materials doped with Nb, Ta, or W; (2) positive temperature coefficient thermistors, $BaTiO_3$ based materials doped with La, Bi, Y, Sb or Ta; and (3) voltage dependent resistor or varistors, based on zinc oxide. The common feature of each is the presence of conductive grains separated by insulating grain boundaries.

Minor dopant additions to commercial ferrites are widely used to control their electrical and magnetic properties.[3,4] Of particular concern is the control of eddy current losses in Mn–Zn ferrites. Eddy current losses are due to electrical resistance-losses within the magnetic core caused by alternating electric fields. It is given by

$$P_e = \frac{CB^2f^2}{\rho} \quad (1)$$

where P_e is the eddy current loss, C is the proportionality constant, B is the flux density, f is the frequency, and ρ is the resistivity. Several approaches have been developed to address various aspects of this problem. These include enhancing the resistivity of the grains. The resistivity of the grains can be increased by substitution of Ti^{4+} for the Fe^{2+} ion on the octahedral site in the spinel lattice. The Ti^{4+} ions trap the conduction electrons associated with Fe^{2+} ions which suppresses electron hopping between Fe^{2+} and Fe^{3+}. Other additives that alter the electronic properties by substitution on the cation sublattice, generally the octahedral site, include SnO_2, Sc_2O_3, In_2O_3, Li_2O_3, and V_2O_5.[5]

Eddy current losses can also be minimized by forming uniform, small grain, pore free microstructures. High purity raw materials or additives which suppress grain growth, such as Ta_2O_5, can be utilized to control the grain size.

In the pioneering work, Guillaud[6] reported the effect of calcium addition in reducing eddy current losses in ferrites. The addition of SiO_2 and CaO to MnZn ferrite was reported by Akashi[7] to increase the resistivity and decrease the eddy current loss by the formation of highly resistive grain boundaries. The addition of Ca, usually in combination with SiO_2, has been utilized by numerous authors[4,5,8,9] to control magnetic losses in ferrites.

2 Experimental procedure

Mn ferrites were prepared using standard ceramic processing techniques. Oxides and carbonates of the starting materials were mixed in a polypropylene ball mill with isopropyl alcohol and either calcia stabilized ZrO_2 or steel grinding media for 30 min. The powder was oven-dried at 110°C followed by calcining in air at 1000°C for 4 h in a platinum crucible. The calcined powder was then remilled during which reagent grade SiO_2 and $CaCO_3$ were added, individually or in equal weight percentages. Pellets were uniaxially pressed at 36 MPa in a 1·9 cm die and then sintered in either air or flowing nitrogen at 1250°C for 4 h. The heating rate during sintering was 5°C/min.

Samples sintered in air were cooled either at the rate of −1°C/min or −10°C/min. The samples sintered in flowing nitrogen were cooled at −10°C/min, which was the recommended cooling rate to avoid damage to the furnace tube.

Samples were electroded with sputtered coatings of Au or Au–Pd. Electrode resistance was measured to verify a low resistance before testing. AC impedance response was measured using a commercial low frequency impedance analyzer. DC electrical response of the current versus voltage was measured at voltages below 25 V using a current source to apply between 10 nA and 10 mA to the samples, with the resulting voltage drop measured with an electrometer. The in-line current was monitored with a digital multimeter. Due to I^2R resistive heating of the sample, a pulse technique was utilized at the high fields. The custom designed and built source was capable of producing a rectangular pulse of up to 1000 V for a duration of 1 ms at a frequency of 50 Hz with a maximum current output of 150 A. The pulse applied to the samples was displayed on an oscilloscope and the data manually recorded.

The magnetic Curie temperature varies markedly with composition and the cation distribution between the octahedral and tetrahedral sites for the Mn_3O_4–Fe_3O_4 system. The Curie temperature, therefore, provides a highly sensitive measure of changes in the crystal chemistry of the magnetic phase present.

The use of a thermogravimetric analyzer has been shown to provide a ready technique to measure the Curie temperature.[10] Sintered specimens were placed in the weighing pan of a thermogravimetric analyzer. A permanent magnet was placed on top of the horizontal furnace assembly of the analyzer. The apparent weight of the sample in the magnetic field of the permanent magnet was recorded as a function of temperature for a heating rate of 10°C/min. When the sample was heated through the magnetic Curie temperature, its apparent weight increased due to the loss of the spontaneous magnetization. The magnetic Curie temperature, was arbitrarily defined as the maximum of the temperature derivative of the apparent weight change. All TGA results presented were performed in a magnetic field.

3 Results and discussion

3.1 Impedance results

An electrical analog for the microstructure of ferrites was first presented by Koops[11] where a resistor and capacitor in parallel corresponded to the different phases in the microstructure. Assuming a continuously connected minor phase separating the major phase, the individual RC circuits of similar phases can be combined, which reduces the model to two RC elements, one representing the bulk grains and the other the grain boundaries (Fig. 1A).

Such a circuit can be analyzed using complex impedance spectroscopy. The complex impedance $Z(\omega)$ of an ideal system at an angular frequency ω may be written as the sum of the resistance $R(\omega)$ and the reactance $\chi(\omega)$:

$$Z(\omega) = R(\omega) + j\chi(\omega) \tag{2}$$

If one plots the imaginary part of the impedance versus the real part, i.e. $R(\omega)$ versus $\chi(\omega)$ the resulting plot shows distinction features for certain combination of circuit elements. For an ideal combination of a resistor and capacitor in parallel, the resulting plot will show a semicircle

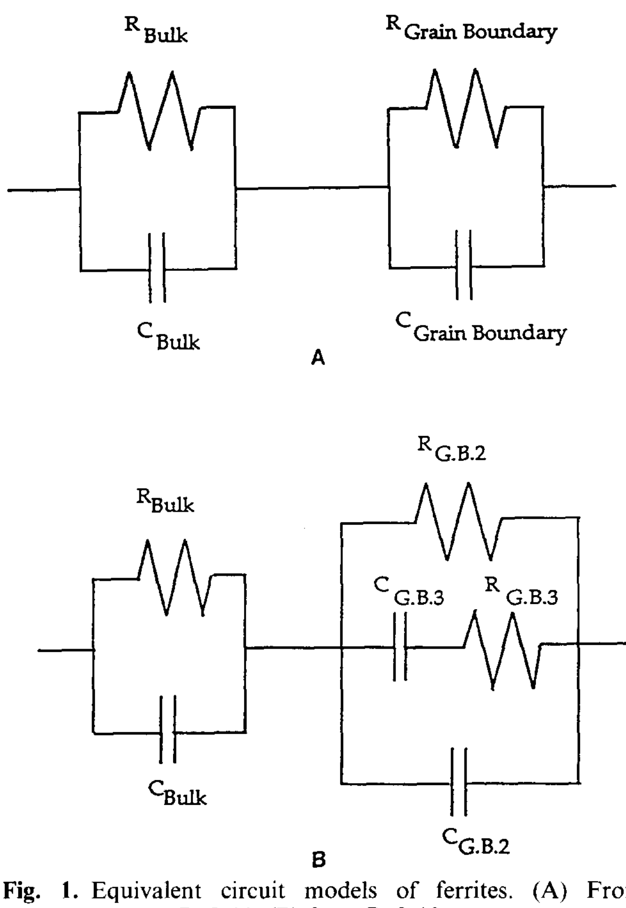

Fig. 1. Equivalent circuit models of ferrites. (A) From Ref. 11, (B) from Ref. 12.

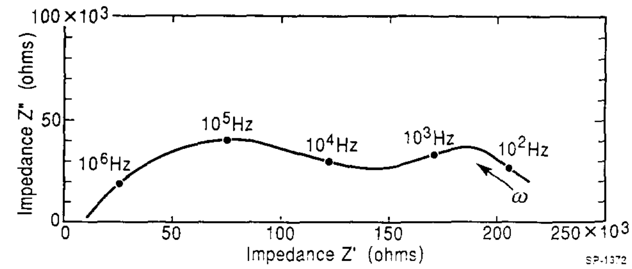

Fig. 2. Complex impedance response of MnZn ferrite with no additions cooled at −1°C/min in air.

located with the locus on the horizontal axis and the high frequency intercept at the origin.

For the specific equivalent circuit of Koops[11] containing two parallel RC circuit elements in series, and providing that the RC time constants of the two RC series elements of the circuit are significantly different, the expected complex impedance representation would be two semicircles, a low frequency semicircle representing grain boundary process and a high frequency semicircle representing the bulk process. The intercepts with the real axis directly correspond to the resistance of bulk (R_{Bulk}) and the sum of resistances of the bulk and grain boundaries ($R_{\mathrm{Bulk+GB}}$) The Koops[11] model was modified by Miroshkin *et al.*[12] who added a series RC leg in parallel with the grain boundary component which he attributed to grain boundary charging (Fig. 1B).

Although Mn–Zn ferrites are of greater commercial interest, the high resistance corresponding to the bulk grains dominated their overall impedance response (Fig. 2). The high resistance of the bulk made it difficult to measure the effect of dopants at the grain boundaries. In order to resolve the response of the grain boundaries to minor dopant additions, the Mn ferrite system with lower bulk resistivity than the Mn–Zn ferrite system was chosen for this study (Fig. 3). One should note that the overall resistance of Mn ferrite was over an order of magnitude smaller than Mn–Zn ferrite and that the bulk and grain boundary components of the complex impedance plot were readily distinguishable.

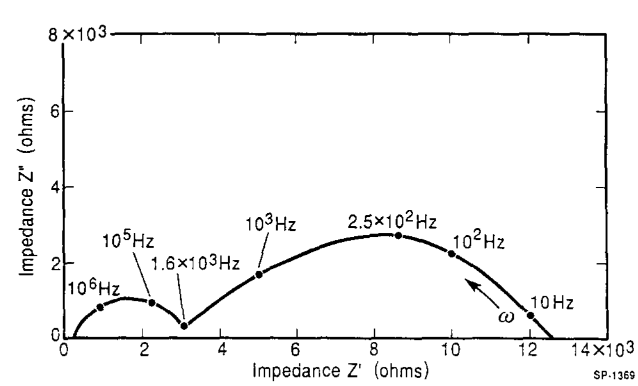

Fig. 3. Complex impedance response of Mn ferrite with no additions cooled at −1°C/min in air.

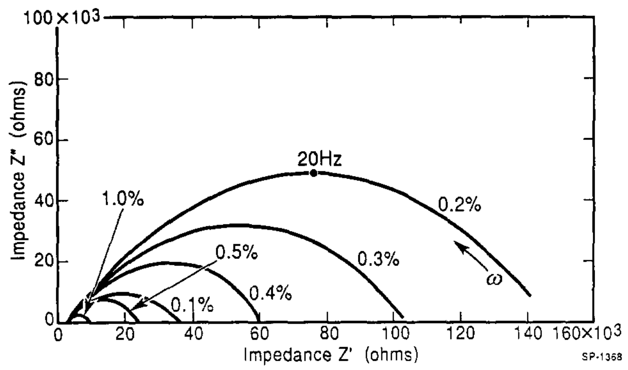

Fig. 4. Complex impedance response of Mn ferrite with between 0·1 wt% and 1·0 wt% SiO_2 and $CaCO_3$ additions, cooled at −10°C/min in air.

The grain boundary component of the impedance for Mn ferrites with additions of up to 1·0 wt% SiO_2 and $CaCO_3$ are shown in Fig. 4. The grain boundary component dominated the total response in every case and the bulk component showed very little sensitivity to the addition of Si and Ca compared to the grain boundary component. Only the low frequency arc corresponding to the grain boundary is shown. The grain boundary resistance varied by more than an order of magnitude for the composition range, going through a maximum between 0·2 wt% and 0·3 wt% SiO_2 and $CaCO_3$ (Fig. 5). (It should be noted that the data from Fig. 3 are incorporated in the 0% addition category.) A maximum in the grain boundary resistance with concentrations of less than 1 wt% is consistent with Akashi's[7] results for Si and Ca additions to Mn–Zn ferrites. This is also similar to other ceramic systems such as ZnO (Ref. 13) and $BaTiO_3$ (Ref. 14) where the electrical properties are critically dependent on dopant concentrations and the maximum response occurs with less than 1% additions.

Mn ferrite samples were also fabricated with between 0·2 and 1·0 wt% additions of $CaCO_3$ only. The low frequency arc corresponding to the grain boundaries are shown in Fig. 6. As with samples containing both SiO_2 and $CaCO_3$ additions, the

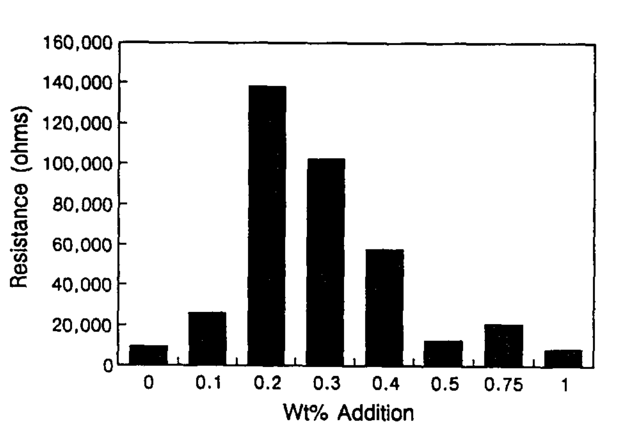

Fig. 5. Electrical resistance of Mn ferrite with between 0·0 wt% and 1·0 wt% SiO_2 and $CaCO_3$ additions, cooled at −10/min in air.

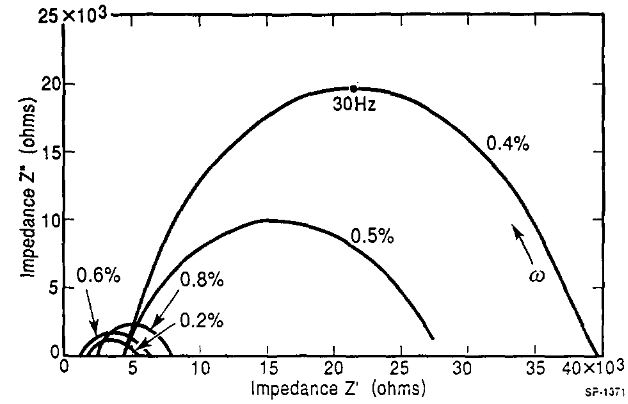

Fig. 6. Complex impedance response of Mn ferrite with 0·2 wt% and 0·8 wt% additions of $CaCO_3$ cooled at −10°C/min in air.

resistivity of the grain boundaries varied by more than an order of magnitude and went through a maximum with less than 1·0 wt% additions, especially at 0·4 wt% $CaCO_3$ additions. Again these results are consistent with those of Akashi[7] who reported a maximum in the resistivity with 0·6 wt% CaO additions for Fe-rich Mn–Zn ferrites.

This work showed that the additions of Ca and Si to Mn ferrites are concentrated at the grain boundaries where they yield the widely recognized effect of modifying its resistance.

3.2 Non-ohmic response

A varistor is a non-linear or voltage dependent resistor and is typically represented by the relationship:

$$I = K\,V^{\alpha} \tag{3}$$

where α is a figure of merit of the non-ohmic response of the material. Combining eqn (3) with ohm's law, $V = IR$, yields an equivalent expression for the voltage dependence of resistance in terms of the parameters K and α:

$$R = \frac{I}{K}\,V^{1-\alpha} \tag{4}$$

Commercially available ZnO-based varistors typically operate at greater than 100 V and have values of α between 35 and 50. ZnO varistors are used in many applications including voltage stabilization or pulse suppression in consumer electronics, surge absorption, and as arrestor elements in lighting arrestor.[15] Low voltage varistors, typically based on SiC, used to equalize the direct currents in telephone circuits require α values of greater than 3.[16]

The current versus voltage characteristics of Mn ferrites containing 0·3 wt% SiO_2 and $CaCO_3$ are shown in Fig. 7. On a log–log plot, an ohmic response would correspond to a straight line. At low voltages ohmic behavior was observed and was attributed to the resistance of the grain

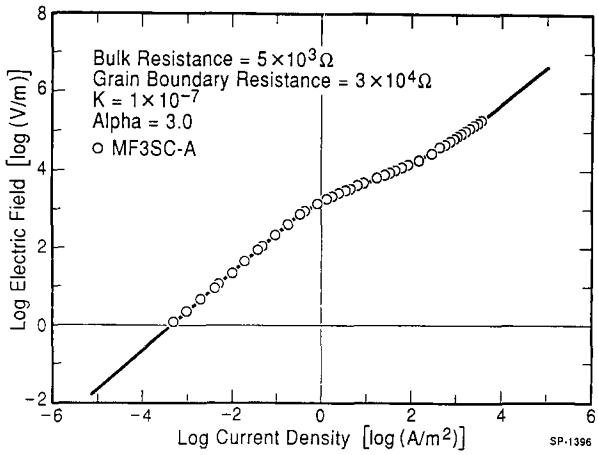

Fig. 7. DC current versus voltage response of Mn ferrites with 0·3 wt% SiO_2 and $CaCO_3$ additions cooled at −10°C/min and the best fit using the equivalent circuit model.

boundaries. At moderate voltages, a non-ohmic region was observed. At high voltages the curve turns upward approaching a second region with linear ohmic response.

When solved for DC conditions, the equivalent circuit of Koops[11] with two parallel RC circuits elements in series, as well as the modified circuit of Miroshkin *et al.*,[12] reduce to a series combination of resistors, with the response at all voltages given by

$$V = I(R_{Bulk} + R_{GB2}) \tag{5}$$

where R_{Bulk} and R_{GB2} refer to the resistance of the bulk and grain boundary, respectively. The current–voltage response of Mn ferrite can not be represented by these models.

A model to represent the observed current–voltage response would require that there are two parallel processes occurring at the grain boundaries, one yielding a voltage-independent component of the resistance, and another yielding a voltage-dependent component of the form of eqn (3). This would be represented by an equivalent circuit similar to that of Miroshkin *et al.*[12] but with the series RC leg of the grain boundary component (R_{GB3}) of the equivalent circuit of Fig. 1(B) replaced by a voltage-dependent resistor of the form of eqn (4) (Fig. 8A). For DC conditions this reduces to the circuit of Fig. 8(B) and can be represented by

$$V = I\left(R_{Bulk} + \frac{R_{GB2}R_{GB3}}{R_{GB2} + R_{GB3}}\right) \tag{6}$$

From the experimental evidence of the complex impedance analysis it was concluded that $R_{GB} \geq R_{Bulk}$. There are two limiting conditions which are readily apparent. At low voltages, from eqn (3) and $R_{GB3} \gg R_{GB2}$, eqn (6) reduces to

$$V = IR_{GB2} \tag{7}$$

At sufficiently high voltages, where $R_{GB2} > R_{GB3}$,

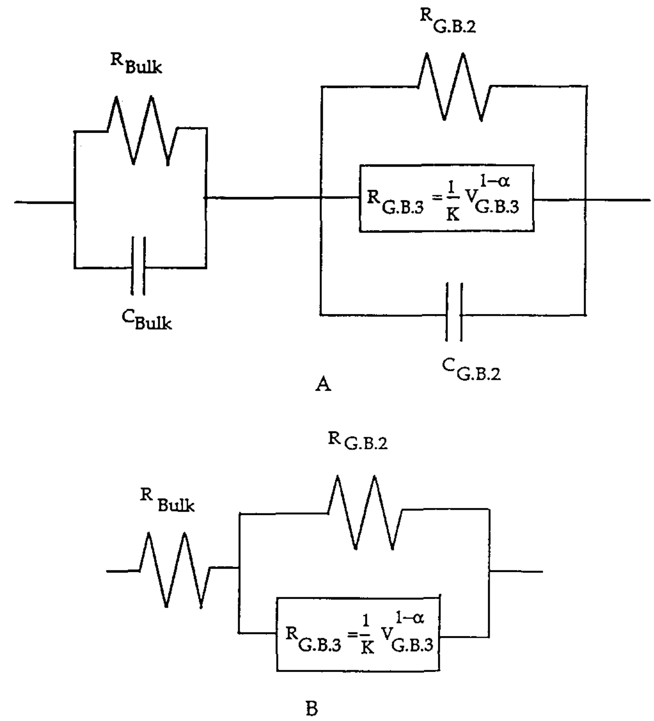

Fig. 8. (A) Equivalent circuit model of Miroshkin *et al.*[12] modified for a non-ohmic resistor; (B) modified model under DC conditions.

eqn (6) reduces to

$$V = I(R_{Bulk} + R_{GB3}) \tag{8}$$

for the condition where $R_{Bulk} > R_{GB3}$, eqn (8) reduces to

$$V = IR_{Bulk} \tag{9}$$

The R_{GB3} in eqn (6) is given by eqn (4) where the voltage is that across the voltage-dependent resistor, V_{GB3}, rearrangement and substitution yields

$$V_{GB3} = V - IR_{Bulk} \tag{10}$$

Substituting eqns (4) and (9) into eqn (5) yields

$$V = I\left(R_{Bulk} + \frac{R_{GB2}\frac{1}{K}(V - IR_{Bulk})^{(1-\alpha)}}{R_{GB2} + \frac{1}{K}(V - IR_{Bulk})^{(1-\alpha)}}\right) \tag{11}$$

The parameters which serve to describe the device are R_{Bulk}, R_{GB2}, α, and K.

Assuming values of I_{GB3} to range from 10^{-10} to 10^{-2} and appropriate R_{Bulk}, R_{GB2}, α and K, I and V can be calculated. The resulting curves for various combinations of R_{GB2}, R_{Bulk}, α, and K are shown in Fig. 9. The curves successfully represented the limiting conditions of eqn (5) discussed above. As the value of alpha was increased, the sharpness of the transition increased. R_{GB2} successfully represented the limiting conditions of eqn (6) where $R_{GB3} > R_{GB2} > R_{Bulk}$, while R_{Bulk} represented the limiting conditions of eqn (7) where R_{Bulk} and

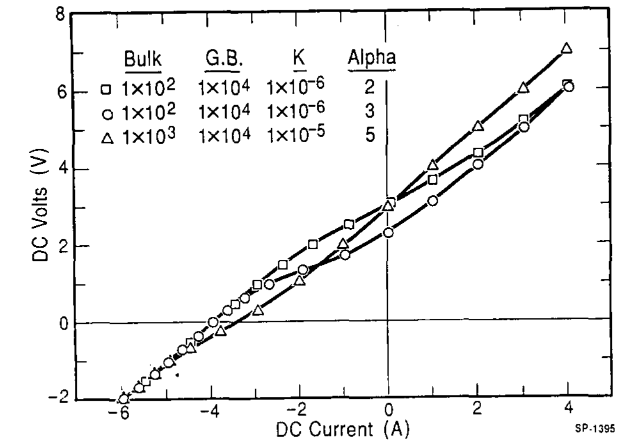

Fig. 9. Calculated current versus voltage response of Mn ferrites for various combinations of the equivalent circuit parameters R_{GB}, R_{Bulk}, K', α.

$R_{GB2} > R_{GB3}$. Therefore, R_{GB2} controls the DC response at low fields, while R_{Bulk} controls the DC response at high fields. Such a transition is not possible using the previous models of either Koops[11] or Miroshkin *et al.*[12]

A numerical iteration technique was used to fit this model to the experimental results. This is shown in Fig. 7 for Mn ferrite with 0·3 wt% SiO_2 and $CaCO_3$ additions. The circles represent the measured current and voltage values, while the solid line represents the best fit of the equivalent circuit model.

The best fit values of the equivalent circuit parameters were determined for Mn ferrite compositions with between 0·0 and 1·0 wt% additions of SiO_2 and $CaCO_3$ cooled at two different rates. The values of the coefficient of non-linearity, α, ranged from 2·0 to 3·0 and went through a maximum between 0·2 and 0·4 wt% additions (Fig. 10). The values of α obtained for Mn ferrites were similar to the 2·1 to 3·5 reported by Kuanr *et al.*[17] and the 1·2 to 5·1 reported by Larson and Metselaar[18] for yttrium iron garnet.

Although the Mn ferrite samples with Si and Ca additions did show some non-ohmic current versus voltage response, the calculated values of α

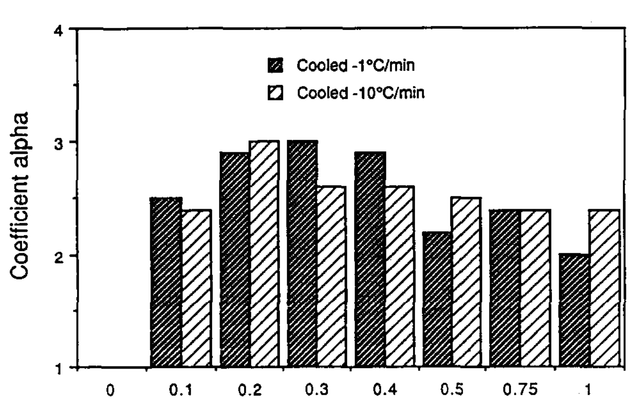

Fig. 10. Coefficient of non-ohmic response of Mn ferrites with various additions of SiO_2 and $CaCO_3$.

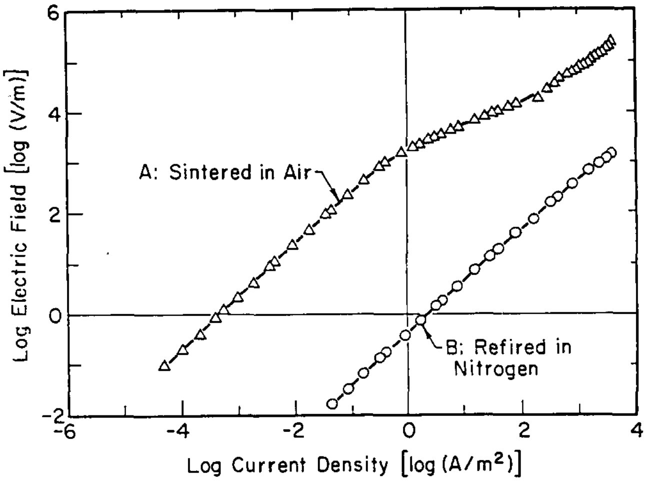

Fig. 11. DC current versus voltage response of Mn ferrites with 0·3 wt% SiO_2 and $CaCO_3$ additions: (A) after sintering in air, (B) after refiring in N_2 at 1250°C for 2h.

were all ≤3, the minimum value necessary for use in telecommunication circuits. Attempts to enhance the ratio of the resistance of the grain boundary to the resistance of the bulk grains were performed by subjecting the samples to high temperature anneals with atmospheres containing various partial pressures of oxygen.

Samples sintered and cooled in air were subjected to a high temperature anneal (1200°C/4h) in a nitrogen atmosphere in an attempt to further decrease the resistance of the bulk grains, as can be seen in Fig. 11, the overall resistance of the sample decreased from 3×10^5 Ω to 50 Ω due to reduction of the sample. The reduction of the sample eliminated the difference of the resistivity between the bulk grains and the grain boundaries and resulted in the elimination of the non-ohmic transition region.

Additional samples of Mn ferrite with 0·3 wt% SiO_2 and $CaCO_3$ additions were fabricated and sintered at 1250°C in flowing nitrogen, and cooled at the cooling rate of the furnace. The samples

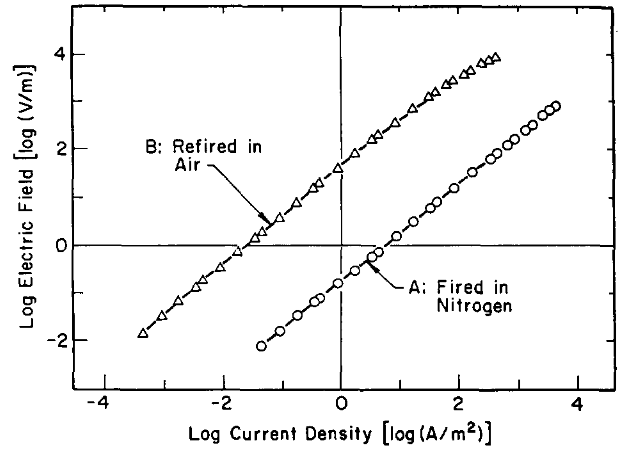

Fig. 12. DC current versus voltage response of Mn ferrites with 0·3 wt% SiO_2 and $CaCO_3$ additions: (A) sintered in N_2, (B) refired in air at 1050°C for 15 min and cooled at −10°C/min.

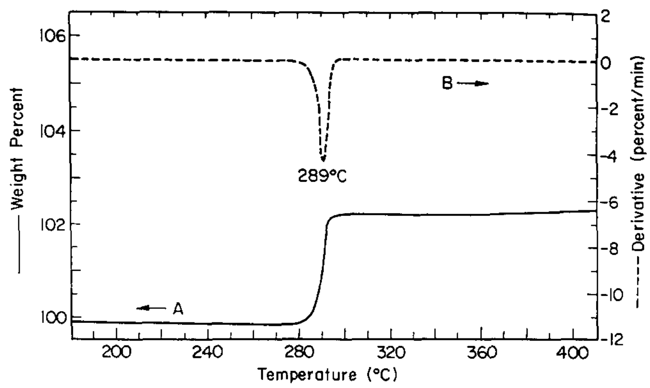

Fig. 13. TGA in a magnetic field of Mn ferrite pellet with no additions sintered and cooled in nitrogen: (A) wt% change, (B) rate of weight change.

were highly conductive (R = 18 Ω) and did not show any non-ohmic response. The samples were subjected to a high temperature (1200°C) thermal anneal in air from 15 to 120 min with the objective of selectively oxidizing the grain boundaries to increase their resistivity, while maintaining the high conductivity of the bulk grain. Although the resistance did increase with longer thermal treatments, no significant non-ohmic response was obtained, Fig. 12.

The difference between the most resistive grain boundary, obtained for a sample with Si and Ca additions sintered in air, and the least resistive bulk, obtained for different samples sintered in nitrogen, was ~10^4 Ω. This difference corresponds to a limiting value for the magnitude of the non-ohmic transition in Mn ferrites. This is in contrast to the >10^{12} Ω transition reported for ZnO.

3.3 Thermal stability

Figure 13 shows a gravimetric thermogram in argon for a nitrogen sintered and cooled Mn ferrite sample without additions. The magnetic transition is sharply defined and the magnetic Curie temperature was 289°C, which is similar to the literature value of 300°C.

Mn ferrite wafers without additions were subjected to various thermal anneals in air using TGA apparatus. Figure 14 shows the sample weight during isothermal anneal for various times at nominal temperature of 600°C, and during subsequent cooling in a magnetic field. Weights are given as a percent of the initial weight. As the duration of the air anneal was increased, several points are readily apparent. The samples showed a progressively increasing weight gain at the annealing temperature. This was attributed to oxidation of the sample. Secondly, the magnetic Curie temperature was shifted following the thermal anneal. For anneals ≤15 min the calculated T_c shifted to slightly higher temperatures. For anneals ≥20 min the T_c were shifted to lower temperatures. Thirdly,

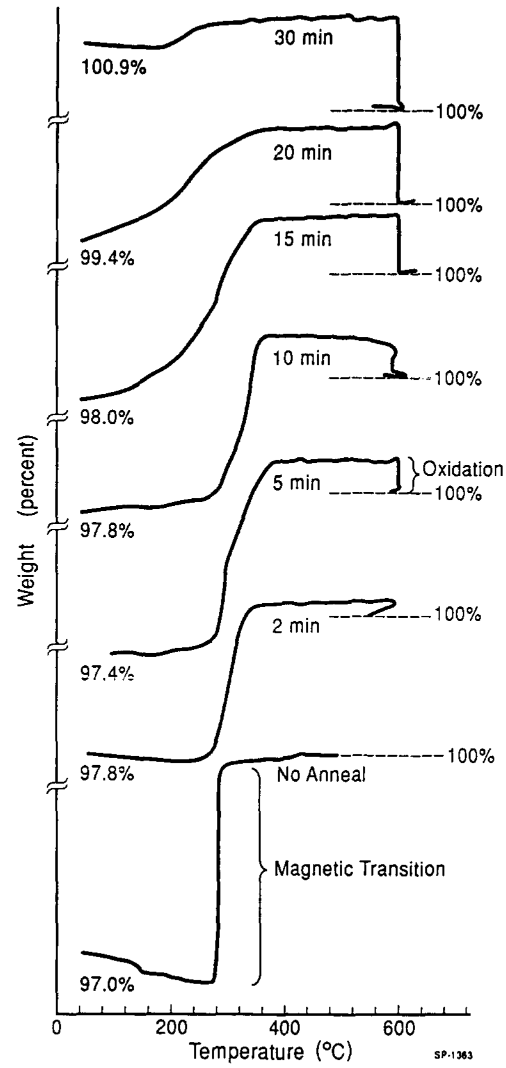

Fig. 14. TGA of Mn ferrites wafers with no additions subjected to various thermal anneals for up to 30 min in air.

the magnetic transition on cooling occurred over progressively wider temperature ranges. For the sample annealed for 20 min the onset of the magnetic transition began at 400°C and was not completed until the temperature was below 100°C. Following an anneal in air for 30 min the magnetic transition occurred over a 200°C temperature range, with the maximum of the derivative of the weight gain placing the T_c at ~225°C.

Upon oxidation in air $MnFe_2O_4$ decomposes into Mn_2O_3 (bixbyite) and Fe_2O_3 (hematite). X-ray diffraction patterns (Fig. 15) shows the initial appearance of bixbyite and hematite after only 2 min of annealing at 600°C, for the samples with no additions. These become the preponderant phases after 30 min.

The very important role of the additives in providing thermal stability to the ferrites was previously reported.[19] Mn ferrite samples containing from 0·2 to 1·0 wt% SiO_2 and $CaCO_3$ were subjected to thermal anneals at 600°C for 2 h, and in contrast to samples without additions, the magnetic transition of the ferrites with additions remained sharply defined indicating no decomposition of

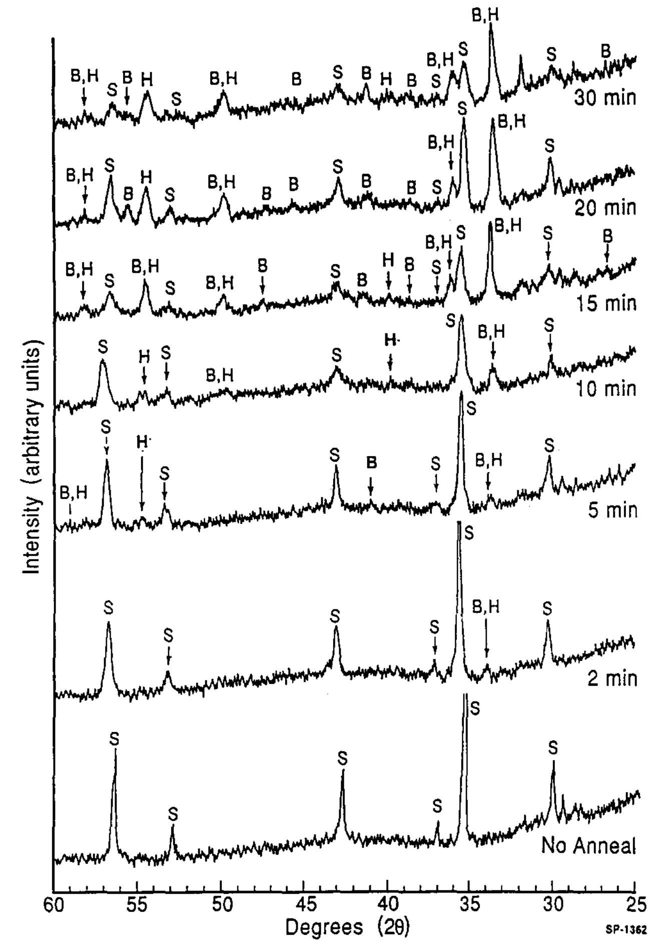

Fig. 15. X-ray diffraction patterns of specimen surfaces of Mn ferrite with no additions subjected to various thermal anneals for up to 30 min in air (Cu Kα radiation), where B is bixbyite, H is hematite, and S is spinel.

the magnetic phase during the thermal anneal in air. The derivative of the weight gain confirmed the sharpness of the magnetic transition (Fig. 16). The very slight shift in the Curie temperature was attributed to a change in the cation distribution and is consistent with the work of Jirak and Vratislav.[20] The suppression of the decomposition of Mn ferrite with SiO_2 and $CaCO_3$ additions was

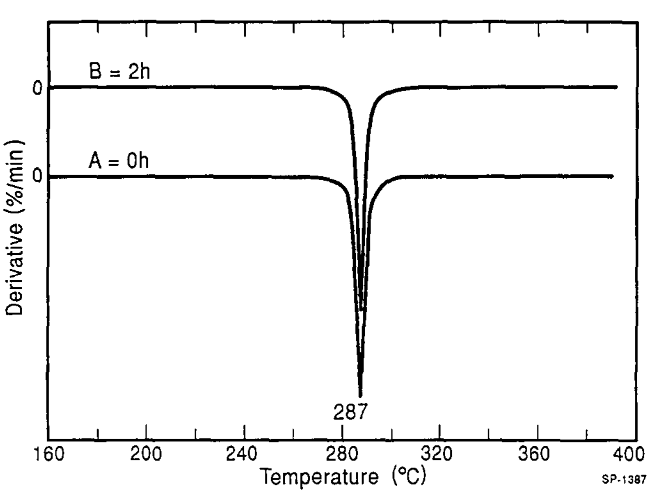

Fig. 16. Derivative of the TGA curve in a magnetic field of Mn ferrite with 0·3 wt% SiO_2 and $CaCO_3$ additions: (A) initial heating (B) cooling following an anneal at 550°C for 2 h in air.

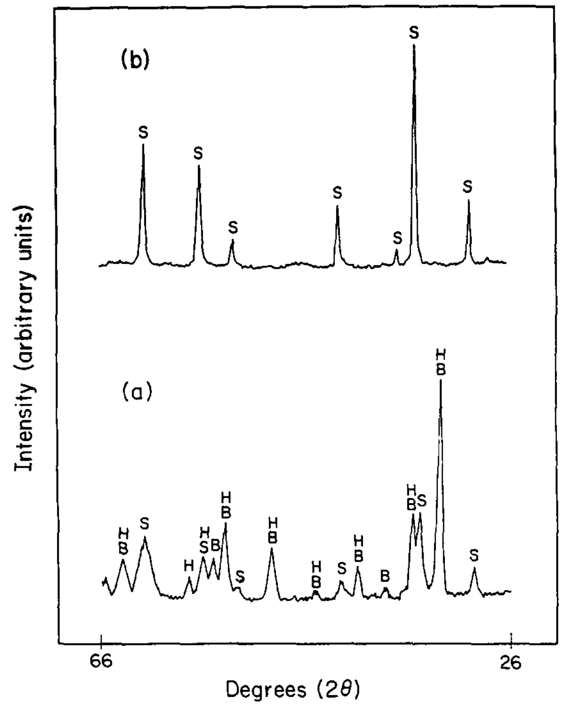

Fig. 17. X-ray diffraction patterns using CuKα radiation of (A) Mn ferrite with no additions annealed in air at 600°C for 4 h; (B) Mn ferrite with 0.3 wt% SiO_2 and $CaCO_3$ additions annealed in air at 500°C for 4 h.

confirmed by XRD analysis which detected only the spinel phase (Fig. 17). This is in dramatic contrast to samples without additions which decomposed under similar thermal treatments. The presence of less than 1·0 wt% of both silica and calcium additions inhibited the oxidation and resulting thermal decomposition.

Therefore, the modifications of the grain boundaries in Mn ferrite by the addition of Si and Ca, decreased the grain boundary diffusion of oxygen and inhibited the oxidation and associated decomposition of the ferrite grains when subjected to a post-sintering thermal anneal in air.

4 Conclusions

The role of minor additions ($x \leq 1{\cdot}0$ wt%) of Si and Ca in modifying the physical and electrical properties of the grain boundaries in manganese ferrites was investigated. The measured resistivity went through a maximum between 0·2 and 0·4 wt%. Although a shift from grain boundary to bulk control of the electrical conductivity was obtained at fields $>10^3$, the calculated values of the coefficient of non-ohmic response, α, was less than 3 for all composition investigated, insufficient for most device applications.

Manganese ferrite decomposed when subjected to post-sintering thermal anneals at temperature below 600°C in air. The addition of less than 1% of SiO_2 and $CaCO_3$ inhibited this phase decomposition. The role of Si and Ca additives in the control of the thermal stability of ferrites may be as important to the overall electrical properties as the previously recognized role in the control of the electrical conductivity of the grain boundaries.

Acknowledgements

One of the authors (J. H. B.) would like to express his gratitude to J. L. Baptista and F. M. B. Marques at the Universidade de Aveiro, Aveiro, Portugal, where a portion of this work was performed with the financial support of a Fulbright Fellowship.

References

1. Levinson, L. M., *Advances in Ceramics* (Vol. 1, Grain Boundary Phenomena in Electronic Ceramics). American Ceramic Society Columbus, OH, USA, 1981.
2. Yan, M. F. & Heuer, A. H., *Advances in Ceramics* (Vol. 17, Additives and Interfaces in Electronic Ceramics), American Ceramic Society, Columbus, OH, USA, 1983.
3. Hendricks, C. R. & Amarakoon, V. W. R., Processing of manganese zinc ferrites in high frequency switch mode power supplies. *Ceramics Bull.*, **70**(5) (1991) 817–23.
4. Ishino, K. & Narumiya, Y., Development of magnetic ferrites control and applications of losses. *Ceramic Bull.*, **66**(10) (1987) 1469–74.
5. Ghate, B. B. Processing and magnetic properties of low loss and high stability Mn–Zn ferrites. In *Material Science Research* (Vol. 11, Processing of Crystalline Ceramics), ed. H. Palmour III, R. F. Davis & T. M. Hare. Plenum Press, New York, USA, (1978), pp. 369–79.
6. Guillaud, C., The properties of manganese–zinc ferrites and the physical processes governing them. In *Proc. of the Inst. of Elect. Eng.* (Vol. 104, Part B Supplement 5). 1956, pp. 165–73.
7. Akashi, T., Effect of addition of CaO and SiO_2 on the magnetic characteristics and microstructures of manganese–zinc ferrites ($Mn_{0.68}Zn_{0.21}Fe_{2.11}O_{4+\delta}$). *Trans Japanese Inst. Metals*, **2** (1961) 171–6.
8. Roess, E., Eddy current and hysteresis losses in manganese zinc ferrites. In *Ferrites: Proceedings of the International Conference*, ed. Y. Hoshino, S. Ida & M. Segiomoto. University of Tokyo Press, Tokyo, Japan, 1979, pp. 187–90.
9. Hishiyama, Y., Kanai, K., Iimura, T., Harada, H. & Sugihara, H. Analysis of loss on Mn–Zn ferrites containing CaO. *Advances in Ceramics* (Vol. 15, Proceedings of the 4th International Conference on Ferrites Part 1), ed. F. F. Y. Wang. American Ceramic Society, Columbus, OH, USA, 1985, pp. 491–6.
10. Walters, D. S. & Wirtz, G. P., Kinetics of cation ordering in magnesium ferrites. *J. Am. Cer. Soc.*, **54**(11) (1971) 563–6.
11. Koops, C. G., On the dispersion of resistivity and dielectric constant of some semiconductors at audiofrequencies. *Phys. Rev.*, **83**(1) (1951) 121–5.
12. Miroshkin, V. P., Panova, Y. I. & Passynkov, V. V., Dielectric relaxation in polycrystalline ferrites. *Phys. Stat. Sol. (a)*, **66** (1981) 779–82.
13. Miyoshi, T., Maeda, K., Takahashi, K. & Yamazaki, T., Effects of dopants on the characteristics of ZnO varistors. *Advances in Ceramics*, (Vol. 1, Grain Boundary Phenomena in Electronic Ceramics) ed. L. M. Levinson. American Ceramic Society, Columbus, OH, USA, 1981, pp. 309–15.
14. Heywang, W., Resistivity anomaly in doped barium titanate. *J. Am. Cer. Soc.*, **47**(10) (1964) 484–90.
15. Matsuoka, M., Progress in research and development in zinc oxide varistors. *Advances in Ceramics* (Vol. 1, Grain Boundary Phenomena in Electronic Ceramics), ed. L. M. Levinson. American Ceramic Society, Columbus, OH, USA, 1981, pp. 290–308.
16. Yan, M. F. & Rhodes, W. W., Varistor properties of (Na, Ba) doped TiO_2. *Proceedings of the Material Research Society Symposium* (Vol. 5, Grain Boundaries in Semiconductors), ed. H. J. Leamy, G. E. Pike & C. H. Seager. Elsevier Press, New York, USA, 1982, pp. 357–62.
17. Kuanr, B. K., Singh, P. K. & Kishan, P., Voltage dependence of DC resistance in polycrystalline ferrimagnetic materials. *J. Appl. Phys.*, **61**(8) (1987) 4379–81.
18. Larson, P. K. & Metselaar, R., Electric and dielectric properties of polycrystalline yttrium iron garnet: space charge limited currents in inhomogeneous solids. *Phys. Rev. B.*, **8**(5) (1973) 2016–25.
19. Boy, J. & Wirtz, G. P., The role of grain boundary modifications in the thermal decomposition of Mn-ferrites. *Proceedings of the NATO Advanced Study Institute, Surface and Interfaces of Ceramic Materials*, ed. L. C. Dufour, C. Monty & G. Petot-Ervas. Kluwer Academic Publishers, Dordrecht, The Netherlands, 1989, pp. 691–9.
20. Jirak, Z. & Vratislav, S., Temperature dependence of distribution of cations in $MnFe_2O_4$. *Czech J. Phys.*, **B 24** (1974) 642–7.